Evaluating an Integration of Spacecraft Location Estimation with Crater Detection Toward Smart Lander for Investigating Moon

Keiki Takadama*, Tomohiro Harada*, Hiroyuki Kamata**, Shinji Ozawa***,
Seisuke Fukuda, and Syujirou Sawai****

*The University of Electro-Communications, Japan
e-mail: {keiki@inf, harada@cas.hc}.uec.ac.jp

**Meiji University, Japan
e-mail: kamata@isc.meiji.ac.jp

***Aichi University of Technology, Japan
e-mail: ozawa@aut.ac.jp

****Japan Aerospace Exploration Agency (JAXA), Japan
e-mail: {fukuda, sawai}@isas.jaxa.jp

Abstract

This paper integrates the spacecraft location estimation method with the crater detection method in the SLIM (Smart Lander for Investigating Moon) mission proposed by JAXA (Japan Aerospace Exploration Agency), and investigates its effectiveness from the viewpoint of a location estimation accuracy and time by matching the craters detected from a camera shot image with those in a crater map created from "KAGUYA" (SELENE) satellite. For this purpose, we conduct the experiments based on the five locations in the crater map on moon, and obtain the following implications: (1) the integrated methods can achieve a high location estimation accuracy even in some inconsistencies between two methods (*i.e.,* the crater size gap and the crater detection error); (2) both the appropriate crater size selection and the increase of the total number of the triangles composed of the detected craters improve the location estimation accuracy but it requires a larger computational time than the target time; (3) the improved search mechanism added in the integrated methods can achieve mostly 100% accuracy of the location estimation while reducing a computational time.

1 Introduction

In the usual planetary landing, a spacecraft generally requires a large landing area without obstacles to land a safe area "where is *easy* to land". This means that the conventional approach is difficult to enable a spacecraft to land at the area which is very close to an exploration target. In such a large landing area, even a rover is hard to surely reach at the exploration target because big rocks, craters, and caves may exist in a high possibility in the way to the target. This approach also requires a huge time to reach an exploration target which increases the mission cost and duration. To overcome this problem, Japan Aerospace Exploration Agency (JAXA) focuses on the *pinpoint landing* on moon and proposed the SLIM (Smart Lander for Investigating Moon) mission which aims at establishing a method of landing the pinpoint area "where is *desired* to land" [8]. This approach enables future landing exploration to land close to a investigating target area. To achieve this goal, it is indispensable for a spacecraft to estimate its current location by sensor data such as a camera shot image, automatically navigate a spacecraft to a target area, and land by avoiding obstacles. One of approaches for such a location estimation is done by matching (a) the crater map created beforehand by the date obtained from "KAGUYA" (SELENE) satellite launched by JAXA [5] with (b) the craters detected from a camera shot image over the moon from the spacecraft.

Toward the spacecraft location estimation for the SLIM mission, our previous research proposed the *ETSM (Evolutionary Triangle Similarity Matching)* method [4, 3] which searches the current spacecraft location by matching the craters detected from the camera shot image with those in the crater map. For the crater detection, Kamata's group proposed the crater detection method based on the Haar-like feature [6]. What should be noted here is that our spacecraft location estimation method and Kamata's crater detection method were independently validated, which means that the integration of these two methods may not work well due to some inconsistencies. Concretely, (1) the crater size in the crater map cannot guarantee to be the same as the one found by the crater detection method because the both sizes are calculated by the different algorithms (*i.e.,* the small gaps may exist in every

craters); and (2) the crater detection method has a possibility of deriving an crater detection error (*i.e.*, some craters are detected even though there are no craters, while other craters are not detected even though there are craters).

From these problems, the aim of this paper is to validate the integrated methods as a whole system from the viewpoint of a location estimation accuracy and time by improving its robustness to both the crater size gap and the crater detection error. For this issue, the following improvements are proposed: (1) an appropriate crater size selection from the crater map; (2) an increase of the total number of the triangles composed of the detected craters (note that the ETSM method marches the craters detected from a camera shot image with those in a crater map in the unit of triangles); and (3) an addition of the improved search mechanism to find the correct location quickly.

This paper is organized as follow. Section 2 explains the overview of the SLIM mission, and Section 3 explains the algorithm of the ETSM method. Section 4 describes the three improvements for both the crater size gap and the crater detection error. Section 5 conducts the experiment and shows their results, and our conclusion is finally given in Section 6.

2 SLIM mission

2.1 Overview

As described in Section 1, the SLIM (Smart Lander for Investigating Moon) mission aims at establishing a method of a *pinpoint landing* on the moon [8]. This mission is planned to carry out by a small spacecraft with a launch weight 400kg (dry weight 100kg). To achieve the pinpoint landing, the following issues should be established: (1) a surface topography matching with a camera shot image, (2) automatically obstacles detection and avoidance, and (3) a landing radar; (4) a reusable landing gear with a memory metal; and (5) a surface exploration rover. This paper particularly tackles (1) a surface topography matching with a camera shot image.

2.2 Spacecraft location estimation in SLIM mission

The landing sequence of SLIM is divided to two phases as shown in Figure 1: (1) the power descent phase and (2) the vertical descent phase. The power descent phase, in particular, is further divided to two phases; (1-i) the inertia guidance phase and (1-ii) the LOS (Line Of Sight) guidance phase. This paper focuses on an estimation of current spacecraft location during (1) the power descent phase and (2) the initial stage of the vertical descent phase.

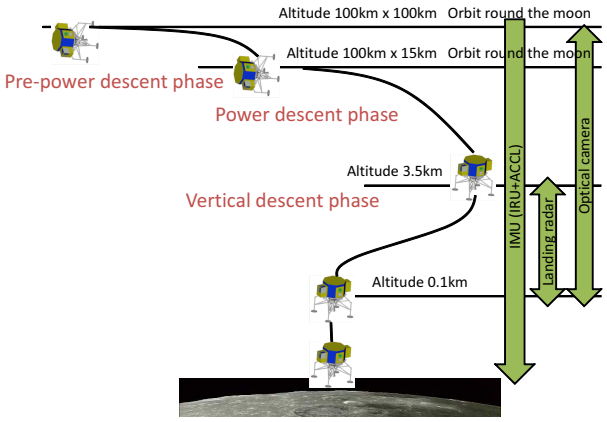

Figure 1. Image of landing sequence in SLIM mission

2.3 Related works on location estimation

In SLIM mission, the location estimation is required in any altitude of the spacecraft because the SLIM spacecraft requires its current location during its descent phase, and such location estimation should be done in real time. From this fact, the location estimation of the SLIM mission requires (1) an estimation in any altitude of the spacecraft, and (2) a short computational time which enables the spacecraft to estimate its location in real time.

Regarding this issue, the conventional location estimation approaches have been proposed. For example, Wertz and Sasaki proposed a star catalog matching with a star pattern given by a star sensor [10][7], while Chen proposed a Fourier-Mellin invariant descriptor and symmetric phase-only matched filter [1]. These conventional approaches, however, do not satisfy the requirement of the SLIM mission. In detail, the work by Wertz and Sasaki cannot cope with the change of an altitude of spacecraft because the detected craters change as an altitude of spacecraft changes while the stars do not change [7][10]. The method by Chen requires huge computational cost to execute image processing [1]. To overcome this problem, our previous research proposed the ETSM method described in the next section.

3 Evolutionary triangle similarity matching (ETSM)

3.1 Overview

The *Evolutionary Triangle Similarity Matching (ETSM)* method [4, 3] estimates a current spacecraft location by matching triangles composed of the detected craters in a camera shot image with those composed of the craters in the crater map created from “KAGUYA” satellite [5]. This matching is evaluated from the viewpoint of the *triangle similarity*.

To understand this method, Figure 2 gives an

overview of the ETSM method. In detail, the ETSM method creates some triangles from the craters detected from a camera shot image (as shown in the left side in Figure 2). In parallel, the ETSM method creates a lot of the candidate locations of the spacecraft represented by the squares (as shown in the right side in Figure 2) in the crater map, and generates four triangles composed of three craters in each candidate location as shown in the middle in Figure 2. Then, one of triangles from a camera shot image is compared with four triangles in each candidate location in the crater map, in order to evaluate whether the compared triangles have the similarity feature. If there is no similarity between the compared triangles, the candidate location changes to new one to search the correct location by *GA (Genetic Algorithm)* [2] as one of evolutionary computation. The features in the ETSM method are summarized as follows: (1) the triangle similarity enables a spacecraft to estimate its location at any altitude or any rotation of the spacecraft; and (2) GA contributes to providing a quick search of the potential location.

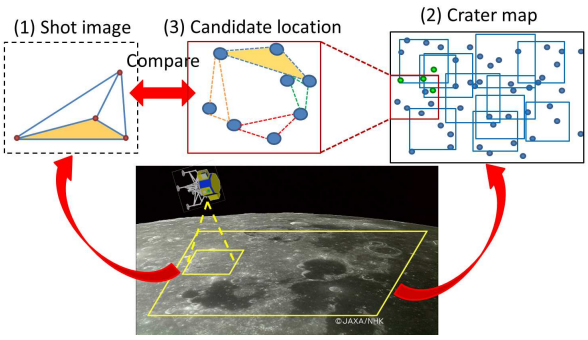

Figure 2. Image of the ETSM method

3.2 Algorithm

The algorithm of the ETSM method is summarized as follows.

1. **Triangle detection from camera shot image:** As shown in Figure 2 (1), the triangles composed of three craters without containing other craters are detected from the camera shot image.

2. **Candidate location creation in crater map:** As shown in Figure 2 (2), a lot of the candidate locations of the spacecraft represented by the squares are created. One square as the candidate location is described as (x, y, l), where the point (x, y) indicates the bottom left corner of the square and a length l indicates one side of the square. As the beginning of this method, the candidate locations are equally arranged on the crater map to cover a whole area, which number is initially configured. From the viewpoint of GA, one square corresponds to an *individual*, and the number of the candidate locations corresponds to *population size* (N_p).

3. **Four triangles creation in candidate location:** As shown in Figure 2 (3), four triangles in each candidate location is created from the top, left, bottom, and right sides.

4. **Evaluation of candidate locations:** To evaluate whether a candidate location is close to the current location, the *interior angles* of the triangles in the camera shot image and those of four triangles in the candidate location are calculated. If the difference of the interior angles between these triangles (*i.e.*, the triangle in the camera shot image and that in the candidate location) becomes zero, then these triangles have a similarity feature. As an evaluation of the candidate location, the minimum difference value of the triangle among four triangles in the candidate location is employed. From the viewpoint of GA, this minimum difference value corresponds to a *fitness*.

5. **Genetic operation:** To search another potential area, two candidate locations are selected by the tournament selection using the finesse value, and one of the following three procedures is executed as shown in 5. of Figure 3.

   - **Crossover operation with the probability $\mathbf{P_c}$:** New candidate locations are generated through the crossover of two selected candidate locations.
   - **Movement operation with the probability $\mathbf{P_m}$:** Two selected candidate locations are moved a little bit toward the triangle having a high fitness value, in order to enlarge a new area (Details are described in Section 4.3).
   - **No operation with the probability $\mathbf{1 - P_c - P_m}$:** No operation is executed.

   Hereafter, we call two new candidate locations (with the probability P_c), two moved candidate locations (with the probability P_m), or two selected candidate (with the probability $1 - P_c - P_m$) as the *target* candidate locations.

6. **Mutation operation:** If the target candidate locations do not have at least one similarity triangle among four triangles, their location change at random as shown in 6. of Figure 3 (Details are described in Section 4.3).

7. **Local search operation:** The target candidate location is compared with its surrounding locations, and the target candidate location changes to the location having the best fitness values among of them as shown in 7. of Figure 3.

8. **Next candidate location generation:** After generating the $N_p - N_r$ number of the target candidate locations by repleting the cycle from 5. to 7. steps, the N_r number of the best old candidate locations remains and the other ($N_p - N_r$ number of) old candidate locations are replaced with the target candidate locations as shown in 8. of Figure 3. Note that the number of the remaining candidate locations is initially configured as a number of elites.

9. Return to steps 3. and 4. until finding the location which has at least two similarity triangles among four triangles or exceeding the maximum generation as shown in 9. of Figure 3. Note that the maximum generation is initially configured.

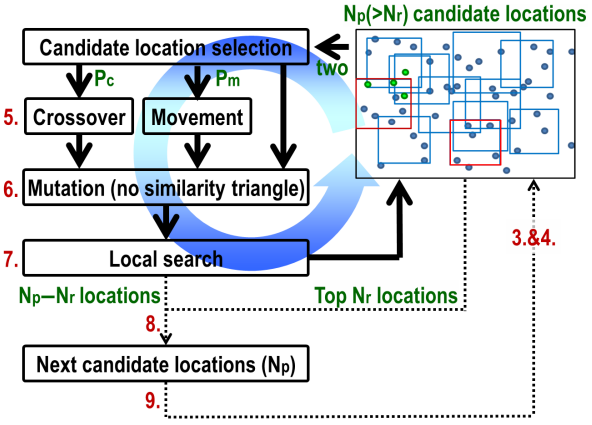

Figure 3. Algorithm of the ETSM method

4 Three improvements

This section describes the three improvements for increasing a robustness to both the crater size gap and the crater detection error, which are occurred by integrating the spacecraft location estimation method with the crater detection method.

4.1 (1) Crater size selection

As described in Section 1, the crater size in the crater map cannot guarantee to be the same as the one found by the crater detection method because the both sizes are calculated by the different algorithms. Figure 4 shows the number and size of the craters in a certain area, where the vertical axis indicates the *number* of the craters while the horizontal axis indicates the *size* of the craters. In detail, the blue bars indicates the number and size of the craters found by the crater detection method, while the orange bars indicates those in the crater map created from "KAGUYA" satellite. This figure suggests that the size of the craters found by the crater detection method is estimated larger than that in the crater map.

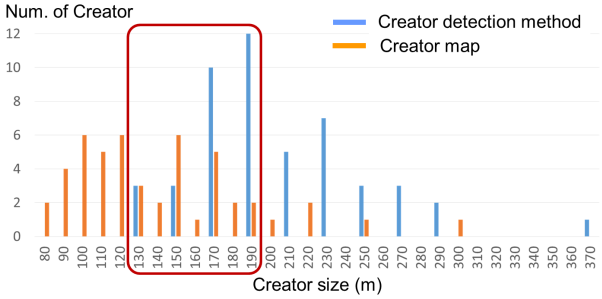

Figure 4. Crater size between crater detection method and crater map

To tackle this crater size gap, we select the crater size from 130 (m) to 190 (m), which are mostly overlapped between the crater detection method and the crater map. This range of the selection is determined from the minimum crater size founded by the crater detection method (*i.e.*, 130 (m) in this case) to the crater size which number is largest or second largest founded by the crater detection method (*i.e.*, 190 (m) in this case). Precisely, the upper crater size is set as the larger crater size among two craters (*i.e.*, 190 (m) or 170 (m)) which number are largest (*i.e.*, 12) and second largest (*i.e.*, 10).

4.2 (2) Increase of triangles composed of detected craters

As the crater detection error, some craters are detected even though there are no craters, while other craters are not detected even though there are craters. In Figure 5(a), the left figure indicates that four triangles (respectively composed of the craters 1, 2, 7, the craters 2, 3, 4, the craters 4, 5, 6, and the craters 6, 7, 8) are extracted as the correct crater detection. However, these detected triangles change as shown in the middle of Figure 5(a) when the craters 4 and 7 cannot be detected, indicating that the only two triangles (respectively composed of the craters 1, 2, 3 and the craters 5, 7, 8) are extracted. This often occurs as the actual crater detection. In addition to this problem (*i.e.*, the decrease of the number of extracted triangles), these triangles tend to have one large angle (such as more than 170 degree), which makes it difficult to distinguish with others. This means that it is very hard to match with the correct triangles. Hereafter, we call the triangle having one large angle as the *bad* triangle shown in the middle of Figure 5(a), while we call the triangle *not* having one large angle as the *good* triangle.

To overcome the problem of decreasing the number of the extracted triangles while increasing the *bad* triangles, this paper proposes the method that extracts four triangles

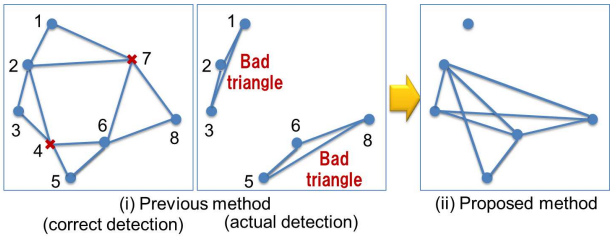

(a) Previous method vs. proposed method

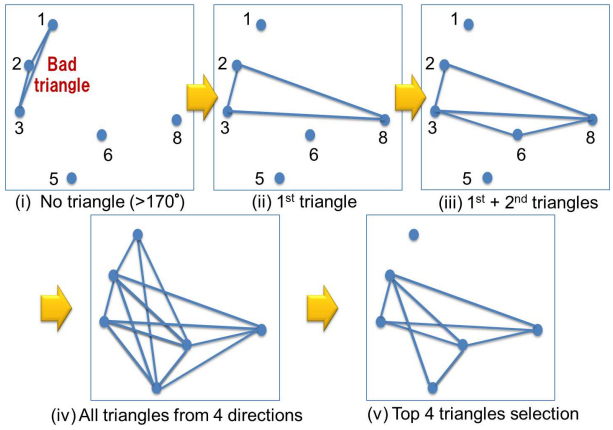

(b) Flow of proposed method

Figure 5. Triangles composed of detected craters

by excluding the *bad* triangles as shown in the right side of Figure 5(a). The algorithm of this method is summarized as follows and its flow is shown in Figure 5(b). Note that Figure 5(b)(i) is the same situation as the middle of Figure 5(a), *i.e.*, the six craters are detected while the two craters cannot be detected.

(i) One triangle is detected by three craters from the upper side (*i.e.*, the craters 1, 2, 3) and is checked whether the triangle has one large angle;

(ii) If the detected triangle has one large angle, then another triangle is detected by using the next three craters from the upper side (*i.e.*, the craters 2, 3, 8) and is checked from the same viewpoint. This step is continued until the good triangle (*i.e.*, the triangle *not* having one large angle) is detected;

(iii) The previous step is continued until the second good triangle is detected;

(iv) Since the above two detected triangles are composed of the craters from the upper size, the same procedure is executed to detect the first and second good triangles from the left, bottom, and right sides. After this step, the eight good triangles (which may be overlapped each other) are finally detected in total;

(v) The top four good triangles are selected among the eight good ones from the viewpoint of a high similarity degree calculated in the past matching.

4.3 (3) Addition of improved search mechanism

Both the crater size gap and the crater detection error described above make it hard to find the correct location, which increases its search time. To reduce a calculation time, this paper proposes the following two types of the location search as shown in Figure 6.

(a) When the candidate location *has* at least one similarity triangle (represented by the red line), the candidate location in the previous method is moved *gradually* as shown in the left side of Figure 6(a), while that in the proposed method is moved *drastically* to search new area quickly as shown in the right side of Figure 6(a). Concretely, the candidate location (represented by the black dash line) which detects the similarity triangle in the upper side is moved to the area (represented by the green dash line) where the same similarity triangle is located at the bottom as shown in the right side of Figure 6(a). Such a large movement enables a spacecraft to search new areas quickly, which contributes to reducing the time for searching the correct location.

(b) When the candidate location does *not have* the similarity triangle, the candidate location in the previous method is moved *at random* as shown in the left side of Figure 6(b), while that in the proposed method is moved *closely* to the similarity triangle detected in the other candidate location as shown in the right side of Figure 6(b). Such a concentrated movement enables a spacecraft to find the correct location quickly, which contributes to reducing the its search time.

5 Experiment

5.1 Cases

To evaluate the integration of the spacecraft location estimation method (ETSM) with the crater detection method (using Haar-Like Feature), we conduct the experiments based on the five locations in the crater map on moon as shown in Figure 7, which is taken from "KAGUYA" satellite at the altitude of 15km. In Figure 7, the points indicate the craters, the five squares indicate the areas where the spacecraft is planned to estimate its location in the SLIM mission. In the experiment, the following cases are conducted as shown in Table 1 to investigate the effectiveness of the following improvements: (1) an appropriate crater size selection from the crater map; (2) an increase of the total number of the triangles composed of the detected craters; and (3) an addition of the improved search mechanism to find the correct location quickly.

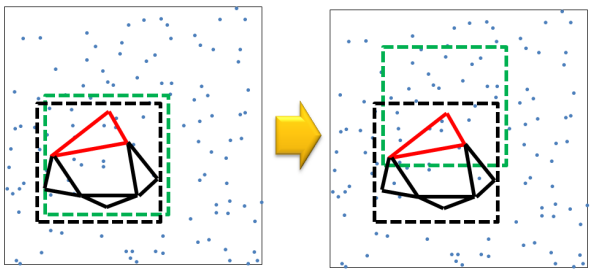

(a) Large movement

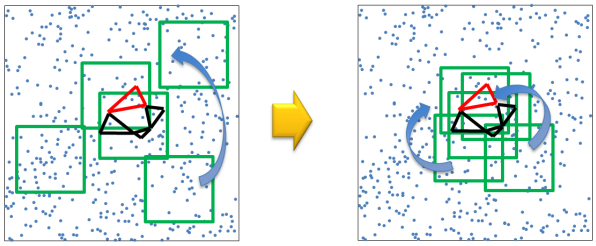

(b) Concentrate movement

Figure 6. Improved search mechanism

Table 1. Experimental cases

Case 1	(1)
Case 2	(1)+(2)
Case 3	(1)+(2)+(3)

5.2 Evaluation criteria and parameter setting

The following evaluation criteria are employed: (1) a success rate in 100 trials and (2) an average estimated time for finding the correct location in 100 trials. In this experiment, the spacecraft location estimation is completed when finding the location which contains at least two similarity triangles. To calculate the estimated time for finding the correct location, we start to obtain the results of *SUZAKU-V* (a CPU board) [9] developed by Atmark Techno, Inc., and then convert the calculation time by obtained SUZAKU-V into the time by the tested environment for the SLIM mission. The specification of both of SUZAKU-V and the tested environment are summarized in Table 2.

The parameters are set as shown in Table 3. Concretely, 25 (= 5×5) candidate locations are initially generated to cover a whole area. The crossover and movement operations are respectively executed with 45% probability. When the old candidate locations are replaced with the new ones, the five best old candidate locations remain as the elite selection. The maximum generation is set as 100.

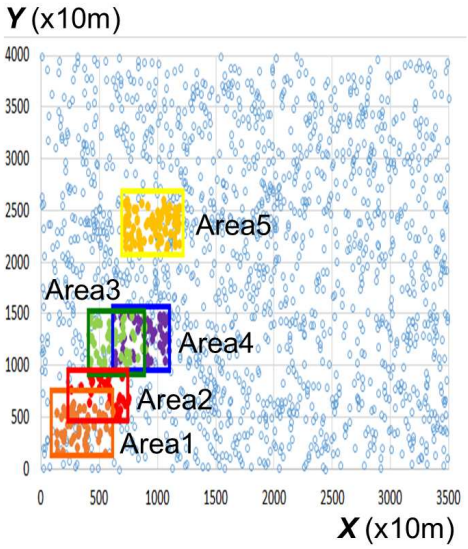

Figure 7. Crater map at an altitude of 15km

5.3 Experimental results

Figure 8(a) shows the experimental result of case 1, where the horizontal axis indicates the five areas while the vertical axis indicates the success rate in 100 trials. The yellow bars indicate the success rate. Figure 8(b), on the other hand, shows the experimental result of cases 2 and 3, where the horizontal axis and the left vertical axis have the same meaning of Figure 8(a) and the right vertical axis indicates the average estimated time in 100 trials. The blue and red bars respectively indicate the success rates of cases 2 and 3, while the blue and red lines respectively indicate their average estimated time.

The result shown in 8(a) indicates that the success rate differ among fives area in case 1. This means that the only appropriate crater size selection from the crater map has a limitation of finding the correct location. The result shown in 8(b), on the other hand, indicates the success rates mostly achieve 100% except for area 5 in case 2 and mostly achieve 100% in all areas in case 3, while the average estimated time in case 3 is shorter than that in case 2 in all areas. This means that the increase of the total number of the triangles composed of the detected craters contributes to finding the correct location in *mostly all* areas, and an addition of the improved search mechanism contributes to finding the correct location *quickly*. Regarding the computational time, in particular, the generation in cases 2 and 3 is less than 100 which is the initial maximum value, meaning that the computational time becomes short.

The above result reveals that the integration of the spacecraft location estimation method (ETSM) with the crater detection method (using Haar-Like Feature) can mostly achieve 100% in all areas with reducing a calcu-

Table 2. Specification

(a) SUZAKU-V

FPGA	Xlinx Virtex-4 FX
CPU core	PowerPC 405
CPU clock	350MHz
DRAM	32MB × 2
Flash memory	8MB (SPI)
Standard OS	Linux

(b) Tested environment

Family	Space-Grade Virtex-4QV
Device	XQR4VLX200
Package	CF1509
Speed	-10
Maximum frequency	52.383MHz

Table 3. Experimental parameters

Num. of candidate locations (N_p)	25
Crossover rate (P_c)	45%
Movement rate (P_m)	45%
Num. of elites (N_r)	5
Num. of maximum generation	100

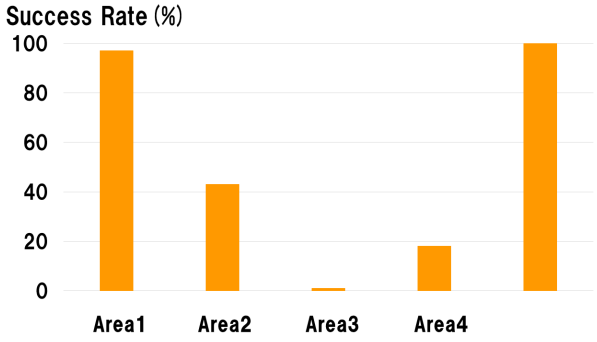

(a) Case 1

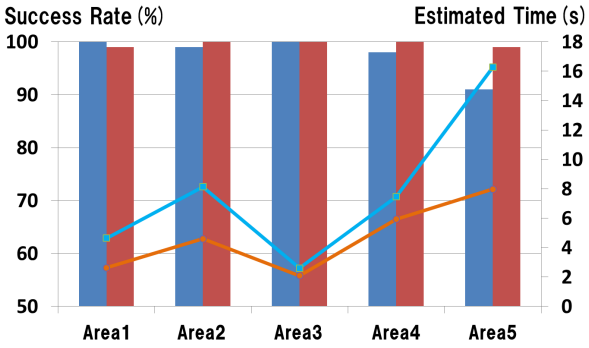

(b) Cases 2 and 3

Figure 8. Success rate and average estimated time

lation time by employing (1) an appropriate crater size selection from the crater map; (2) an increase of the total number of the triangles composed of the detected craters; and (3) an addition of the improved search mechanism.

6 Conclusion

This paper integrated the spacecraft location estimation method with the crater detection method in the SLIM mission in order to validate them together even though such different methods are independently validated in most cases. To investigate an effectiveness of the integrated methods from the viewpoint of a location estimation accuracy and time, the experiments were conducted under the five locations in the crater map on moon taken by "KAGUYA" (SELENE) satellite and have revealed the following implications: (1) the integrated methods can achieve a high location estimation accuracy even in some inconsistencies between two methods (*i.e.*, the integrated methods improved the robustness to both the crater size gap and the crater detection error); (2) both the appropriate crater size selection and the increase of the total number of the triangles composed of the detected craters improve the location estimation accuracy but it requires a larger computational time than the target time; (3) the improved search mechanism added in the integrated methods can achieve mostly 100% accuracy of the location estimation while reducing a computational time.

What should be noticed here is that these results have only been obtained from the five locations in the crater map. Therefore, further careful qualifications and justification, such as an investigation in other locations, are needed to generalize the effectiveness of the proposed methods. These important directions must be pursued in the near future in addition to the following future research: (1) a further reduction of a computational time; and (2) an integration with other crater detection method to improve the location estimation accuracy.

References

[1] Chen, Q. S., Defrise, M., and Deconinck, F.: "Symmetric phase-only matched filtering of Fourier-Mellin transforms for image registration and recognition," *IEEE Transactions on Pattern Analysis and Machine Intelligence*, pp. 1156-1168, 1994.

[2] Goldberg, D. E.: *Genetic Algorithms in Search, Optimization and Machine Learning*, Addison-Wesley, 1989.

[3] Harada, T., Usami, R., Takadama, K., Kamata, H., Ozawa, S., Fukuda, S., and Sawai, S.: "Computational Time Reduction of Evolutionary Spacecraft Location Estimation toward Smart Lander for Investigating Moon," *The 11th International Symposium on Artificial Intelligence, Robotics and Automation in Space (i-SAIRAS2012)*, 2012.

[4] Okamura, R., Harada, T., Usami, R., Takadama, K., Kamata, H., Ozawa, S., Fukuda, S., and Sawai, S.: "Estimate Location by the Evolutionary Triangle Similarity Matching at SLIM," *The 56th Space Sciences and Technology Conference*, 2011 (in Japanese).

[5] Takizawa, Y., Sasaki, S., and Kato, M.: "KAGUYA (SELENE) Mission Overview", *The 26th International Symposium on Space Technology and Science (ISTS)*, 2008.

[6] Tanaami, T., Takeda, Y., Aoyama, N., Mizumi, S., Kamata, H., Takadama, K., Ozawa, S., Fukuda, S., and Sawai, S.: "Crater Detection using Haar-Like Feature for Moon Landing System based on the Surface Image," *The 28th International Symposium on Space Technology and Science (ISTS)*, 2011.

[7] Sasaki, T. and Kosaka, M.: "A Star Identification Method For Star Sensor Attitude Determination Systems By Using Structural Pattern Recognition," *IEEJ Transactions on Electronics, Information and Systems*, Vol. 107, No. 4, pp. 365-372, 1987 (in Japanese).

[8] SLIM Working Group: "A Proposal of Smart Lander for Investigating Moon (SLIM)," JAXA, 2008 (in Japanese)

[9] Atmark Techno, Inc.: *SUZAKU web site*, `http://suzaku.atmark-techno.com` (in Japanese).

[10] J. R. Wertz: *Spacecraft Attitude Determination and Control*, Reidel, 1980.